Journal of Applied Polymer Science

Influence of the Degree of Crosslinking on the Stringiness of Crosslinked Polyacrylic Pressure-Sensitive Adhesives

Keiko Ito,[1] Kohei Shitajima,[1] Nozomi Karyu,[1] Syuji Fujii,[1] Yoshinobu Nakamura,[1] Yoshiaki Urahama[2]

[1]Department of Applied Chemistry, Osaka Institute of Technology, 5-16-1 Ohmiya, Asahi-ku Osaka 535-8585, Japan

[2]Graduate School of Engineering, University of Hyogo, 2167 Shosha, Himeji, Hyogo 671-2201, Japan

Correspondence to: Y. Nakamura (E-mail: nakamura@chem.oit.ac.jp)

ABSTRACT: The stringiness of crosslinked polyacrylic pressure-sensitive adhesive (PSA) was observed during 90° peeling under the constant peel load. The random copolymer of butyl acrylate with 5 wt % acrylic acid crosslinked by *N*,*N*,*N*′,*N*′-tetraglycidyl-*m*-xylenediamine was used as PSA. All observed stringiness upon peeling was sawtooth-shaped, but it could be classified into three types dependent on the degree of crosslinking. The typical sawtooth-shaped stringiness with interfacial failure was observed at the relatively higher crosslinker content ranging from 0.008 to 0.016 chemical equivalents (Eq.), where the PSA has high cohesive strength and low interfacial adhesion. The frame formed at the front end of stringiness at the content ranging from 0.002 to 0.004 Eq. Sufficient interfacial adhesion and deformability generate large internal deformation of the PSA layer. Internal deformation occurred preferentially over peeling as a result of front frame formation. The mode of peeling was changed from cohesive failure to interfacial failure in this range of crosslinker content. The sawtooth-shaped with cohesive failure was observed at the lower content ranging from 0 to 0.001 Eq. The PSA has high interfacial adhesion and low cohesive strength, and thus exhibited cohesive failure. The PSA after peeling remained in the shape of belts. It was found that the shape of stringiness is strongly dependent on the balance between the interfacial adhesion and the cohesive strength of PSA. When the sawtooth-shaped stringiness with frame formed, the peeling rate was lowest. This means the peel strength should be the maximum in this shape of stringiness. © 2014 Wiley Periodicals, Inc. J. Appl. Polym. Sci. **2014**, *131*, 40336.

KEYWORDS: adhesives; copolymers; viscosity and viscoelasticity; surfaces; interfaces

Received 14 October 2013; accepted 21 December 2013

DOI: 10.1002/app.40336

INTRODUCTION

Tse[1] and Yang[2] reported that the pressure-sensitive adhesive (PSA) property *T*, namely the adhesion strength is expressed as follows:

$$T = W_a \times B \times D \quad (1)$$

where W_a is the work of adhesion between the PSA and the adherend, and *B* and *D* are related to the viscoelastic properties of the PSA. *B* is dependent on the plateau modulus of the PSA and the *D* increases with the loss modulus. Tack and peel strength are also dependent on these factors.

In a series of studies to clarify the adhesion mechanism of PSA,[3–15] we referred to W_a as the interfacial adhesion and to $B \times D$ as the cohesive strength of PSA. We have also discussed the relative contributions of interfacial adhesion and cohesive strength to tack.[14] For this purpose, a random copolymer of butyl acrylate (BA) and 5 wt % acrylic acid (AA) [P(BA–AA)] was used and crosslinked by the addition of a crosslinker at various content. Tack was measured using a probe tack tester with two different peel rates (1 and 10 mm/s). The peel behavior of the PSA at the probe tip was observed using a high-speed microscope. The cohesive strength of the PSA decreased with the decrease of crosslinking degree and peel rate, and the interfacial adhesion increased with a decrease of the cohesive strength. As a result, the peeling mechanism was changed and dependent on the crosslinking degree as follows. Cavitation occurred within the PSA layer and peeling progressed simultaneously near the location of maximum stress, then peeled off for the PSA at the relatively higher content of crosslinker. The cavitation formed at the edge of the probe even at low stress and spread to the center with an increase of stress. The cavitation was observed all over the probe interface at near the maximum stress, then peeled off at the medium content of crosslinker. Furthermore, fibrillation occurred before peeling off at a low content of crosslinker. The peeling mechanism was thus strongly dependent on the balance between the interfacial adhesion and the cohesive strength of the PSA.

Stringiness is observed at the tip part of peeling during peel testing. Some researchers have investigated the stringiness

phenomenon.[16–24] Kaelble[16] clarified that the stringiness disperses the applied stress concentrated at the tip part of peeling and increases the peel strength. Urahama[17] reported two types of stringiness shape that are dependent on the backing materials of the PSA tape; sawtooth- and honeycomb-shaped. Urahama clarified that the shape of the stringiness is strongly dependent on the interfacial adhesion, the viscoelastic properties of the PSA and the peel rate. However, the influence of the cohesive strength of PSA on the shape of stringiness has not yet been investigated using a PSA with continuous variation of the cohesive strength.

In this article, the influences of the cohesive strength of PSA and the peel load on the shape of stringiness were investigated. Crosslinked P(BA–AA) with various crosslinking degree was used as PSA. The cohesive strength of PSA changes depending on the crosslinking degree. This PSA is the same as that clarified the peeling mechanism in the tack test in detail in our previous report.[14] When the stringiness is observed under the constant peel load, the peel rate changes depending on the resistance to peeling of PSA. The elastic modulus of PSA is strongly dependent on the peel rate because of the PSA is a typical viscoelastic material. Therefore, the stringiness under constant peel rate was also observed by changing the peel load. The influence of the cohesive strength of the PSA on the mechanism of stringiness formation is discussed.

EXPERIMENTAL

Materials

P(BA–AA) with 5 wt % AA (weight average molecular weight [M_w] of 500,000, polydispersity of 4.9, 40 wt % ethyl acetate solution, synthesized by Toagosei Co., Ltd., Tokyo, Japan) was used as a base polymer. *N,N,N′,N′*-Tetraglycidyl-*m*-xylenediamine (Tetrad-X, Mitsubishi Gas Chemical Company, Inc., Tokyo, Japan) was used as a crosslinker. Reagent grade ethyl acetate and toluene were used as solvents.

Sample Preparation

A 1 wt % ethyl acetate solution of the crosslinker was prepared and a predetermined amount was added to the P(BA–AA) solution. Ethyl acetate was added to prepare the solution with the constant concentration of 30 wt % and the mixture was stirred. The amount of crosslinker was in the concentration range from 0 to 0.016 chemical equivalents (Eq.). The solutions were coated on poly(ethylene terephthalate) (PET) sheets (38 μm thick) using an applicator (Baker type, SA-201, Tester Sangyo Co., Ltd., Saitama, Japan). The coated films were heated at 120°C for 3 min to evaporate the ethyl acetate. It was confirmed beforehand that the subsequent weight reduction hardly occur by this drying condition. Paper coated with a silicon release agent was then attached to the surface of the coated film and the film heated at 60°C for 20 h to accelerate the crosslinking reaction. The thickness of the resulting PSA layer was measured using a thickness indicator (Dial thickness gauge H-MT, Ozaki, Tokyo, Japan) and was determined to be approximately 50 μm.

The PSA solution was also cast on a silicone release agent-coated PET sheet to prepare specimens for measurement of the gel fraction and for tensile tests.

Gel Fraction

The ca. 50 μm thick PSA films cast on a silicone release agent-coated PET sheet were cut into squares (50 × 50 mm) and peeled off. The films were wrapped in PET mesh (#200) and the surrounding area was sealed with a stapler. The prepared specimens were immersed in toluene at 23°C–25°C for 10 days. The swollen films were then dried at 110°C for 3 h. The gel fraction was calculated in accordance with below equation in the same way as the previous report:[13]

$$\text{Gel fraction} = \frac{w_1}{w_0} \times 100. \quad (2)$$

Here w_0 and w_1 are the weights of unswollen and redried specimen, respectively.

Tensile Properties

The square (50 × 50 mm) 50 μm thick PSA films were rolled up to prepare cylindrical samples. The cylindrical samples were then tested using a tensile testing machine (AG-5KNIS, Shimadzu Corp., Kyoto, Japan) with a chuck distance of 10 mm and a tensile rate of 300 mm/min to obtain stress–strain curves in the same way as the previous report.[13]

Peel Strength

A fused quartz plate (50 × 100 × 2 mm) as an adherend was washed with acetone and then with toluene using an ultrasonic washing machine, and finally dried. The prepared PSA tapes were cut into 25 mm wide strips and a strip was then placed onto the fused quartz plate. The strip of PSA tape on the adherend was pressed using a 2 kg iron roller (90 mm diameter, rubber-coated surface) to develop good contact between the PSA and adherend. Test specimens were subjected to five press cycles, where one press cycle involved the iron roller being moved backward and forward. The peel strength was measured 20–30 min after specimen preparation.

The 180° peel strength was measured at a peel rate of 300 mm/min at 23°C–25°C using a tensile testing machine (AG-5KNIS, Shimadzu Corp., Kyoto, Japan) in accordance with JIS Z 0237 (Japanese Industrial Standards) in the same way as in the previous studies.[3–9]

Observation of Stringiness

The PSA tapes with 25 mm width was placed onto a fused quartz plate adherend and pressed using a 2 kg iron roller. This sample preparation method is the same as that for the peel strength test. The stringiness was observed 20–30 min after specimen preparation.

Figure 1 shows the apparatus used for stringiness observation and the part measured for stringiness. The apparatus shown in Figure 1(a) was designed and assembled in-house. Although the observation of stringiness for various peeling angles is possible using this apparatus, only the 90° peeling was observed in this study. A weight was hung at the tip of the adhered PSA tape. One weight is 20 or 200 g and these are equivalent to the applied force of about 0.2 and 2 N. The weight was connected in series and loaded. The stringiness was observed using a digital microscope (TG3000PC, Edenki Inc., Kyoto, Japan) for upper, side, and front views when the peeling is in a stationary state. The peel rate was calculated from the time taken for the

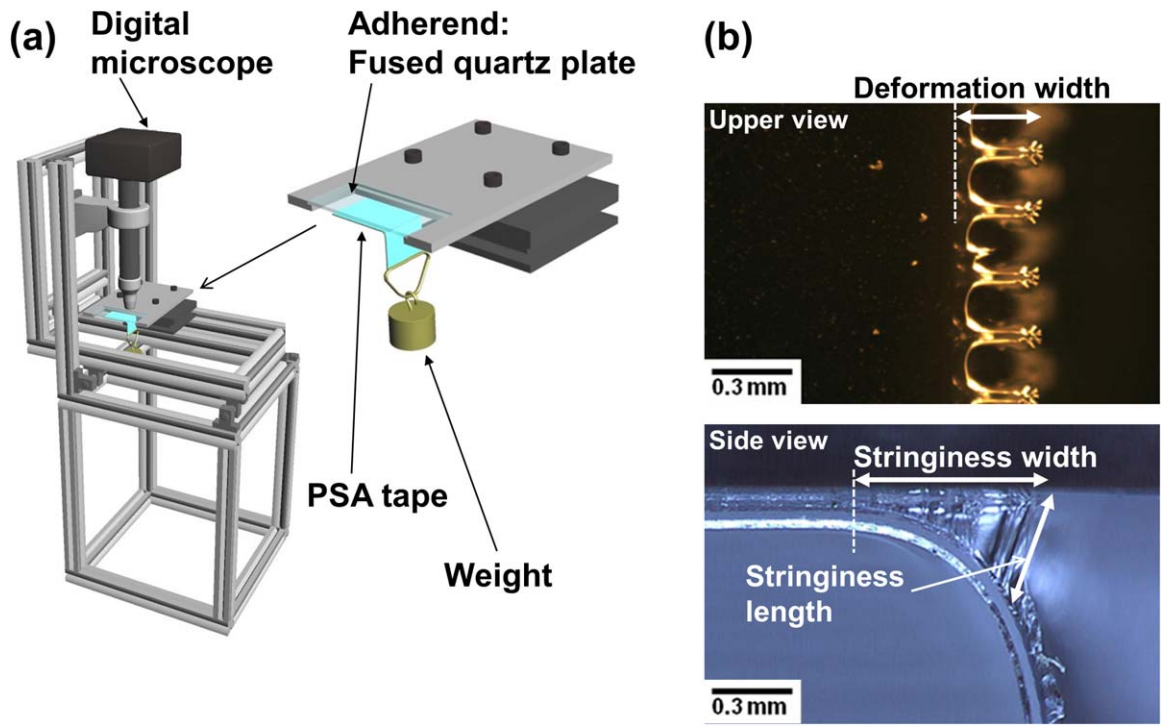

Figure 1. (**a**) Schematic diagram of the apparatus for observation of the stringiness of PSA tapes with 90° peeling and (**b**) the measured dimensions of stringiness. [Color figure can be viewed in the online issue, which is available at wileyonlinelibrary.com.]

stringiness to progress a constant distance. The length of stringiness is clearly observed from the upper view, which is referred to as the deformation width. The stringiness width and stringiness length were measured from the side view, as shown in Figure 1(b).

RESULTS AND DISCUSSION

Gel Fraction

The gel fraction of crosslinked P(BA–AA) is shown in Figure 2. The gel fraction increased with the content of crosslinker above 0.002 Eq., which indicates that the crosslinking points formed were effectively dependent on the crosslinker content.

In order to confirm the difference of the crosslinking degree by changing of crosslinker content, the measurement of degree of swelling is more desirable. However, it was not able to measure the exact degree of swelling in particular at low crosslinker content. So, the gel fraction was measured in this study.

Tensile Properties

Stress–strain curves of crosslinked P(BA–AA) are shown in Figure 3. The tensile rate was 300 mm/min. The non-crosslinked and low-crosslinked (0.001 Eq.) PSAs exhibited greater fracture strain and low stress. For crosslinker content >0.002 Eq., the fracture stress increased, while the fracture strain decreased with an increase of crosslinker content. Thus, the cohesive strength

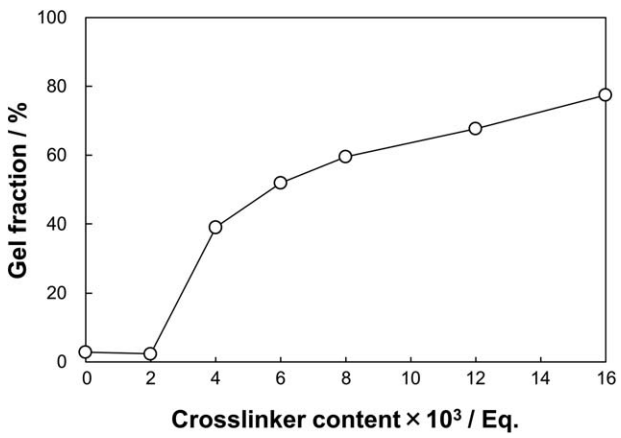

Figure 2. Influence of crosslinker content on the gel fraction of crosslinked P(BA–AA).

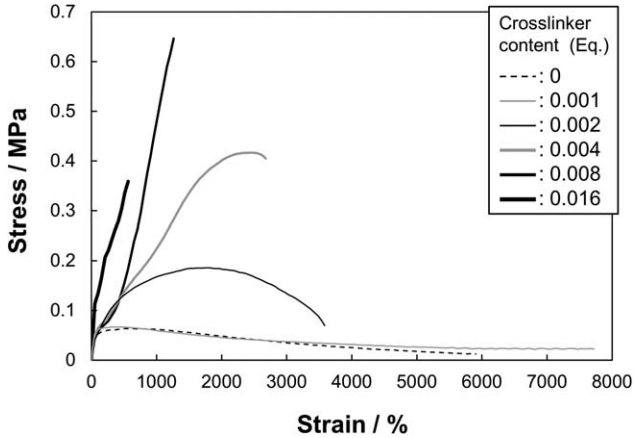

Figure 3. Stress–strain curves of crosslinked P(BA–AA) with various crosslinker content. The tensile rate is 300 mm/min.

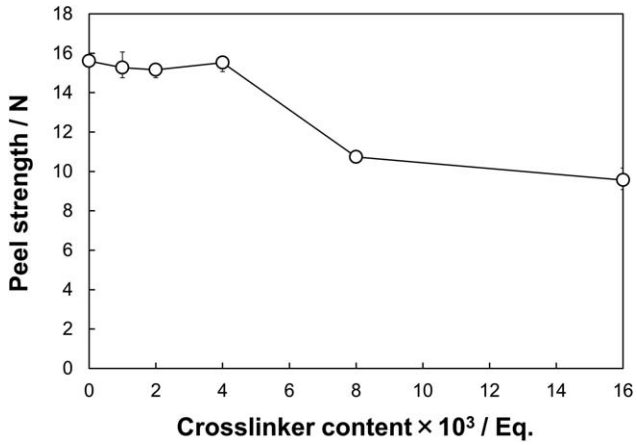

Figure 4. Effect of crosslinker content on the peel strength of crosslinked P(BA–AA). The peel rate is 300 mm/min.

increases, whereas the deformability decreases with an increase in the content of crosslinker.

[Figure 3]

Peel Strength

The influence of crosslinker content on the 180° peel strength is shown in Figure 4. The adherend used was fused quartz plate and the same as that used for stringiness observation. All peeling was interfacial failure and independent of the crosslinker content. The peel strength was higher in the crosslinker content range from 0 to 0.004 Eq. and decreased with >0.008 Eq. due to lower interfacial adhesion. The peel rate was 300 mm/min; therefore, this result cannot be compared directly with the stringiness results discussed later.

Stringiness Under Constant Peel Load

Figure 5 shows digital microscope images for the stringiness of crosslinked P(BA–AA) with various crosslinker content under a constant peel load of 1.2 N. The crosslinker content and the measured peel rate are indicated in each image. The mode of peeling was determined visually to be cohesive failure in the crosslinker content range from 0 to 0.002 Eq. (a–c), and interfacial failure for >0.004 Eq. (d–f). All samples exhibited sawtooth-shaped stringiness, but these were classified into three types that were dependent on the crosslinker content. For crosslinker contents of 0 (a) and 0.001 Eq. (b), long belt-like parallel lines of PSA with equal intervals were observed. A trace of the sawtooth-shaped stringiness was left on the quartz plate surface because the peel mode was cohesive failure (termed "cohesive failure type" hereafter). For crosslinker contents of 0.002 (c) and 0.004 Eq. (d), the frame that connects the tip of each protuberance was clearly evident (termed "front frame type" hereafter). The tip part of each protuberance has more small branches for 0.002 Eq. (c). The peel mode was changed from cohesive failure to interfacial failure in this region. At crosslinker contents of 0.008 (e) and 0.016 Eq. (f), typical sawtooth-shaped stringiness, as previously reported, was observed,[16,17,20–24] where

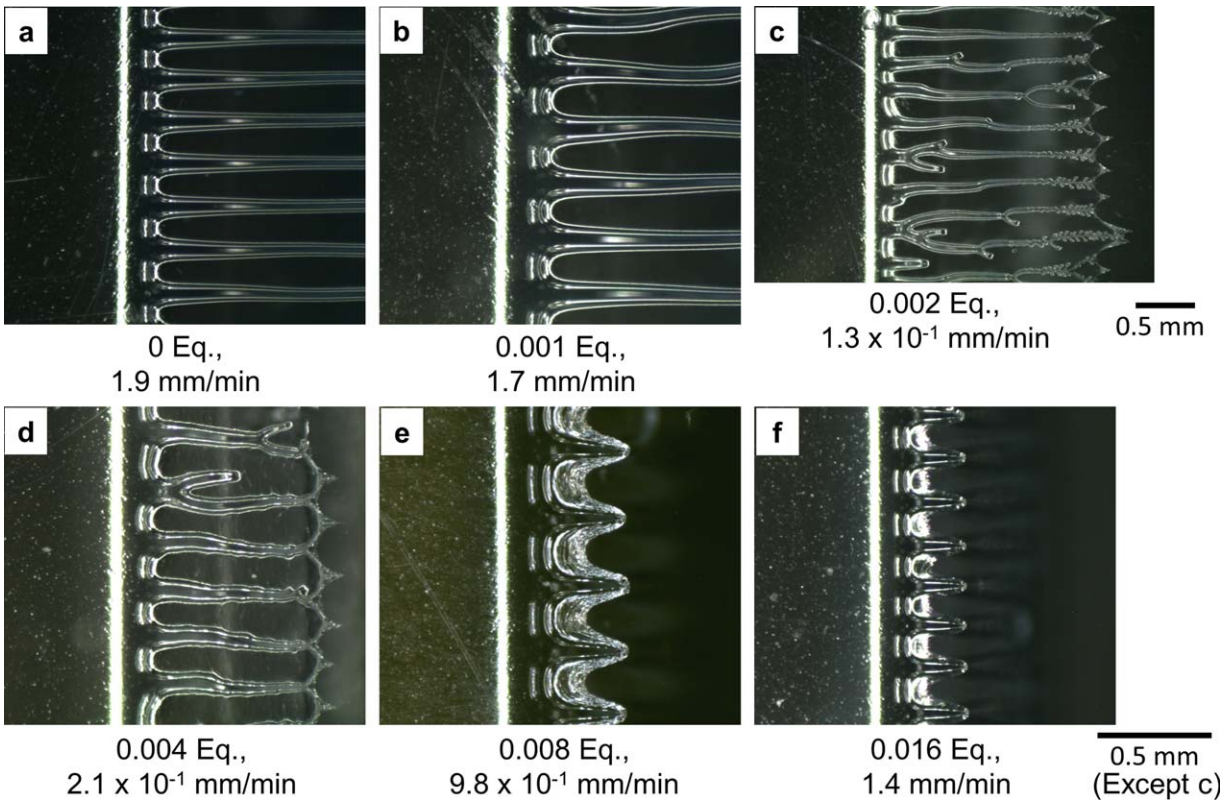

Figure 5. Upper views of stringiness during 90° peeling of crosslinked P(BA–AA) with various crosslinker content under a constant peel load of 1.2 N. The crosslinker content and the actual peel rate are shown under each image. [Color figure can be viewed in the online issue, which is available at wileyonlinelibrary.com.]

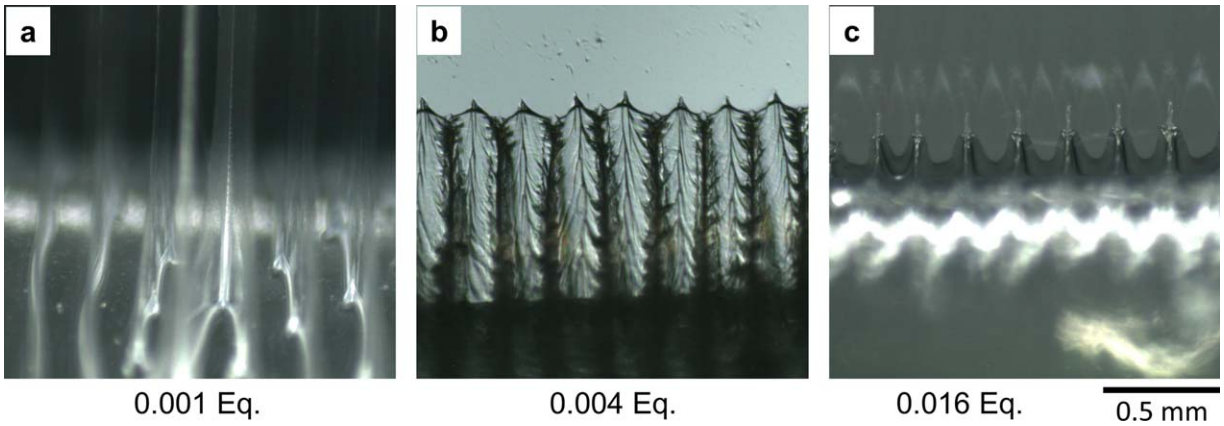

Figure 6. Front views of stringiness during 90° peeling of crosslinked P(BA–AA) with various crosslinker content under a constant peel load of 1.2 N. The crosslinker content is shown under each image. [Color figure can be viewed in the online issue, which is available at wileyonlinelibrary.com.]

the peel mode was interfacial failure. Duckfoot-like webbing was observed at the bottom part between protuberances. The size of the web decreased with an increase of the crosslinker content (e → f) and no front frame was observed (termed "typical type" hereafter).

Figure 6 shows front views of the stringiness with evidence of cohesive failure, that is, the extending and cutting of stringiness was observed for 0.001 Eq. of crosslinker [Figure 6(a), cohesive failure type]. The front frame observed from the upper surface [Figure 5(d)] was continuous and connected to the PSA tape surface for a crosslinker content of 0.004 Eq. [Figure 6(b), front frame type]. Duckfoot-like webbing was clearly observed at the bottom part between protuberances for 0.016 Eq. of crosslinker [Figure 6(c), typical type].

The measured peel rates during stringiness observation under constant peel load were different as indicated for each image. The influences of crosslinker content on the measured peel rate and deformation width are shown in Figure 7. The peel rate and deformation width are inversely proportional and indicate the resistance to peeling. Therefore, they should correspond well with the peel strength. The PSA with a crosslinker content of 0.002 Eq. should have the highest peel strength under these testing conditions; however, the peel mode was cohesive failure. Therefore, the PSA with a crosslinker content of 0.004 Eq., which exhibited interfacial failure, is the most desirable for practical use.

Stringiness Under Constant Peel Rate

The previous section presented the stringiness under constant peel; however, each peel rate was different, as shown in Figure 7. The PSA is a typical viscoelastic material, so that the elastic modulus is strongly dependent on the peel rate. The stringiness under constant peel rate was investigated. Preliminary tests were conducted where various loads were used and the peel rate for each was measured. The relation between the (logarithmic) peel rate and the applied peel load is shown in Figure 8. The linear relation is not obtained between the peel rate and the applied load. This reason is the elastic modulus of PSA changed with the peel rate, because PSA is a typical viscoelastic material as mentioned above. The PSA with 0.002 Eq. of crosslinker required the largest peel load and that for 0.004 Eq. was the second largest. From these results, the ideal peel rate was determined to be 2.6 mm/min (0.42, logarithmic; dashed line in

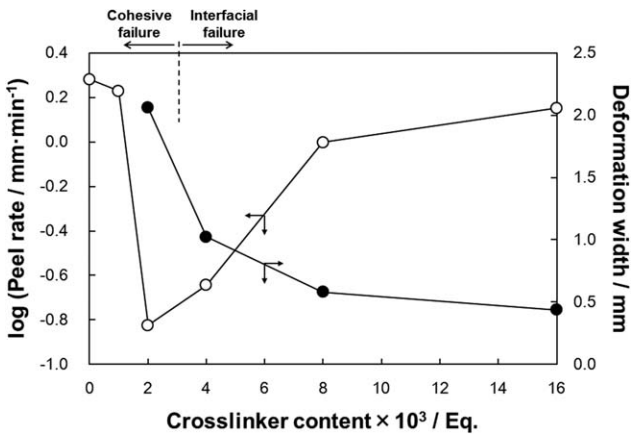

Figure 7. Influences of crosslinker content on the peel rate and deformation width during 90° peeling of crosslinked P(BA–AA) under a constant peel load of 1.2 N.

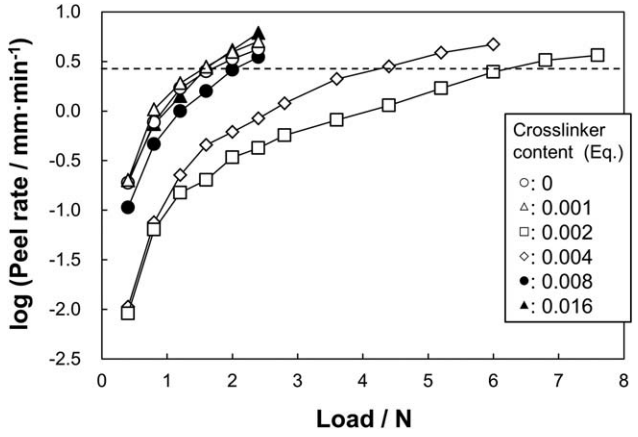

Figure 8. Influence of peel load on the peel rate during 90° peeling of crosslinked P(BA–AA) with various crosslinker content. The *dashed line* indicates the selected peel rate of 2.6 mm/min (0.42, logarithmic) for the observation of stringiness under constant rate.

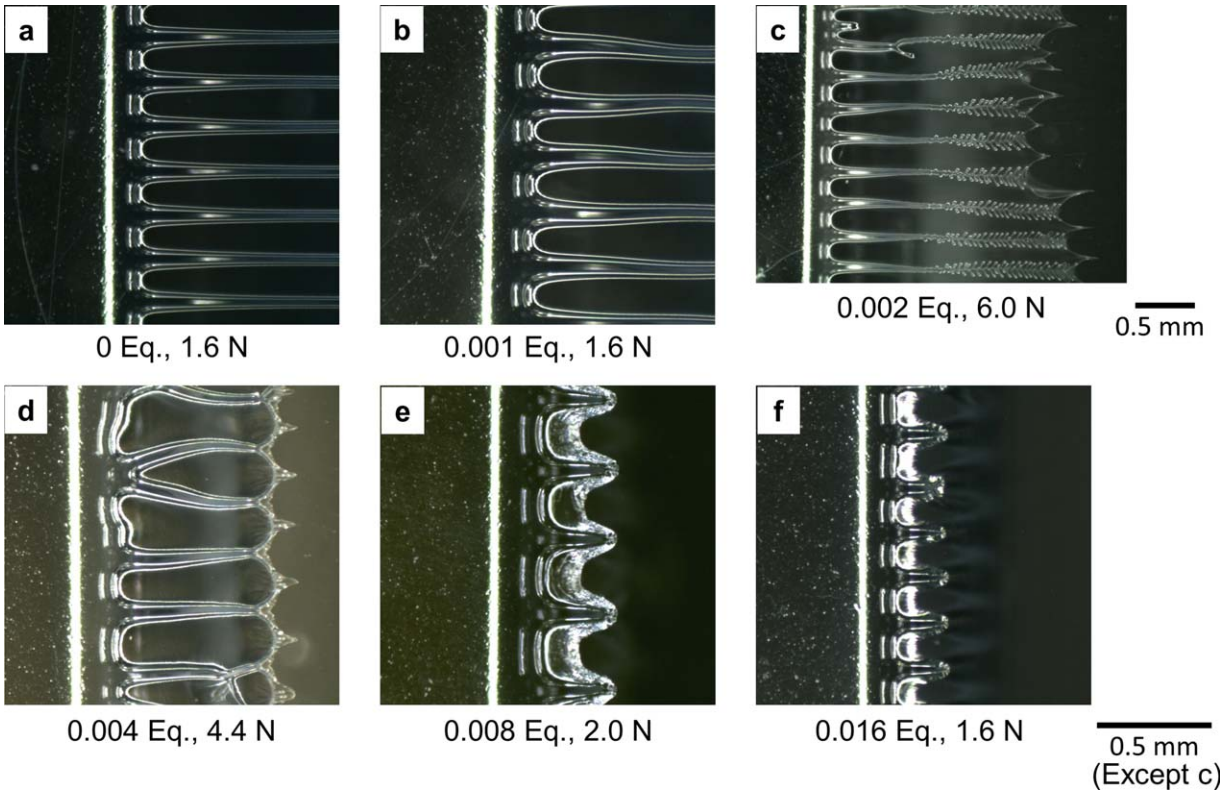

Figure 9. Upper views of stringiness during 90° peeling of crosslinked P(BA–AA) with various crosslinker content under a constant peel rate of ca. 2.6 mm/min. The crosslinker content and the peel load for constant peel rate are shown under each image. [Color figure can be viewed in the online issue, which is available at wileyonlinelibrary.com.]

Figure 8) for the constant peel rate test and the peel load that shows the peel rate closest to 2.6 mm/min was used.

Figure 9 shows digital microscope images for the stringiness of crosslinked P(BA–AA) with various crosslinker content under a constant peel rate of ca. 2.6 mm/min. The crosslinker content and peel load are indicated with each stringiness image. The actual peel rates were (a) 2.8, (b) 2.5, (c) 2.5, (d) 2.7, (e) 2.6, and (f) 2.7 mm/min, respectively. The peel mode was cohesive failure for the crosslinker content range from 0 to 0.002 Eq. (a–c), and interfacial failure for that with >0.004 Eq. (d–f). There was no significant difference between the stringiness shape under a constant peel rate (Figure 9) and those under constant peel load (Figure 5).

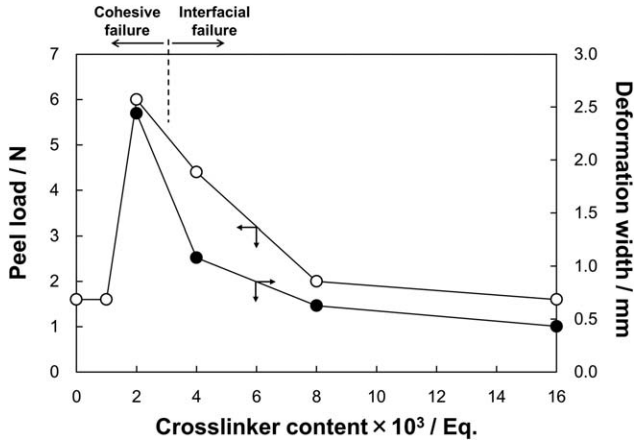

Figure 10. Influences of crosslinker content on peel load and deformation width during 90° peeling of crosslinked P(BA–AA) under a constant peel rate of ca. 2.6 mm/min.

The relation between the peel load required for the constant peel rate (ca. 2.6 mm/min) and the deformation width is shown in Figure 10. The deformation width values for 0 and 0.001 Eq. were not able to measure. The peel load and the deformation width showed similar tendencies with respect to the crosslinker content. Therefore, the peel load for constant peel rate indicates the resistance to peeling and it should thus correspond well with the peel strength.

Technically, the observation of stringiness at 300 mm/min of the standard rate for peel test is possible. However, in this study, it was observed under low peel load, low peel rate, and a stationary state in order to observe the stable stringiness and to confirm the influence of crosslinking degree on the stringiness shape.

Influence of Peel Rate

The influence of peel rate on the stringiness shape was discussed. In the case of crosslinker contents of 0 and 0.001 Eq., the peel mode was cohesive failure for all measured peel rates. The similar cohesive failure type was observed independent of peel rate. Therefore, there was no influence of peel rate on the stringiness shape.

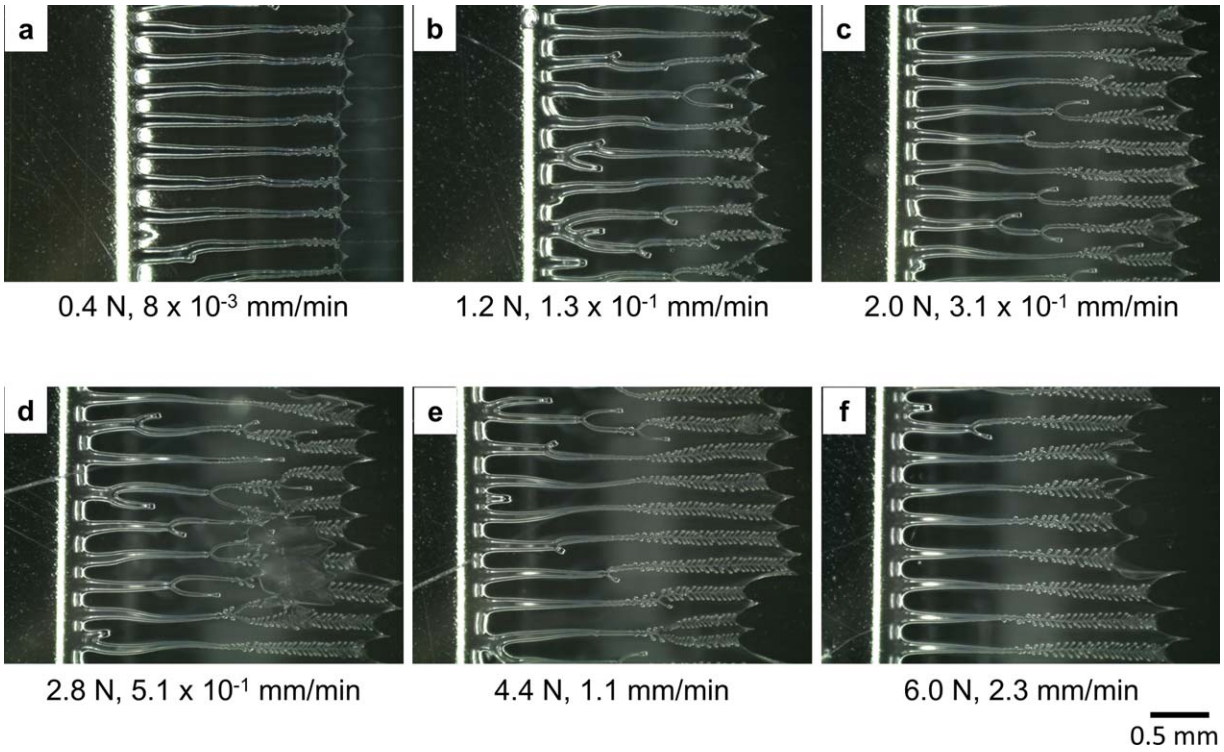

Figure 11. Upper views of stringiness during 90° peeling of crosslinked P(BA–AA) under various peel loads with a constant crosslinker content of 0.002 Eq. The peel load and the actual peel rate are shown under each image. [Color figure can be viewed in the online issue, which is available at wileyonlinelibrary.com.]

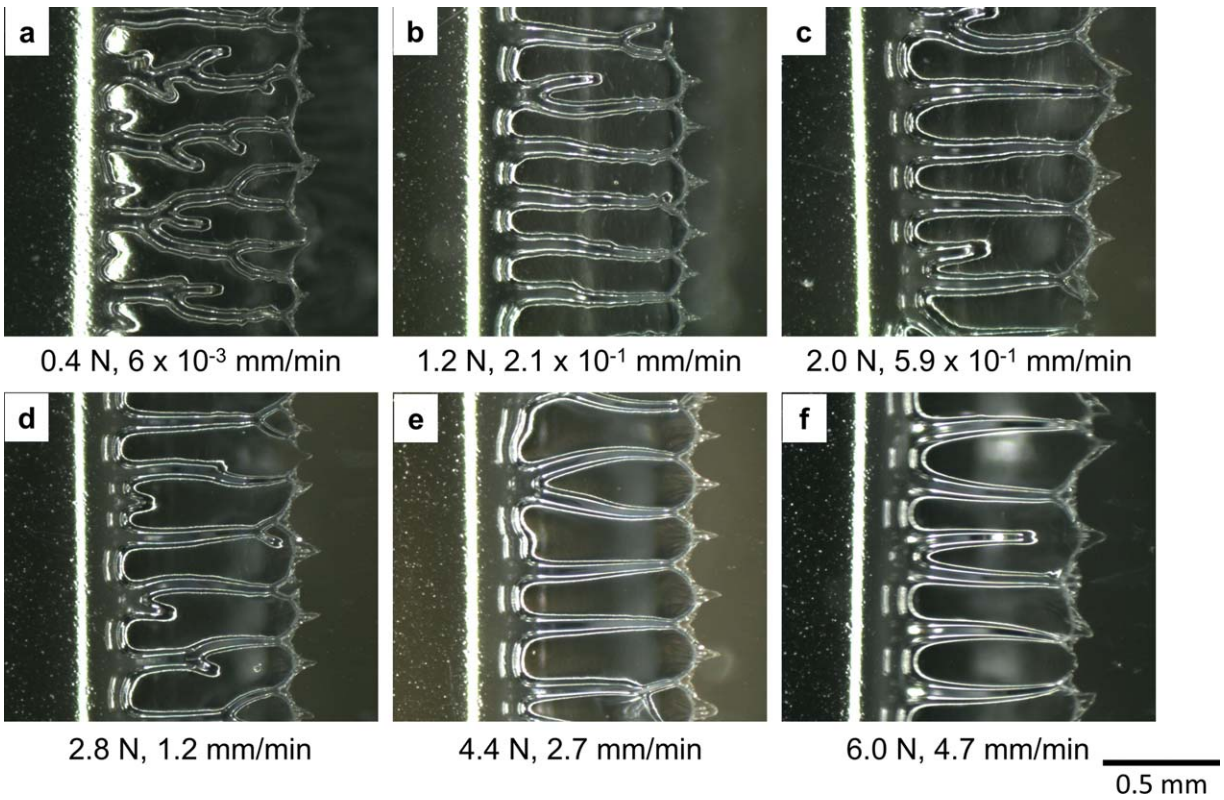

Figure 12. Upper views of stringiness during 90° peeling of crosslinked P(BA–AA) under various peel loads with a constant crosslinker content of 0.004 Eq. The peel load and the actual peel rate are shown under each image. [Color figure can be viewed in the online issue, which is available at wileyonlinelibrary.com.]

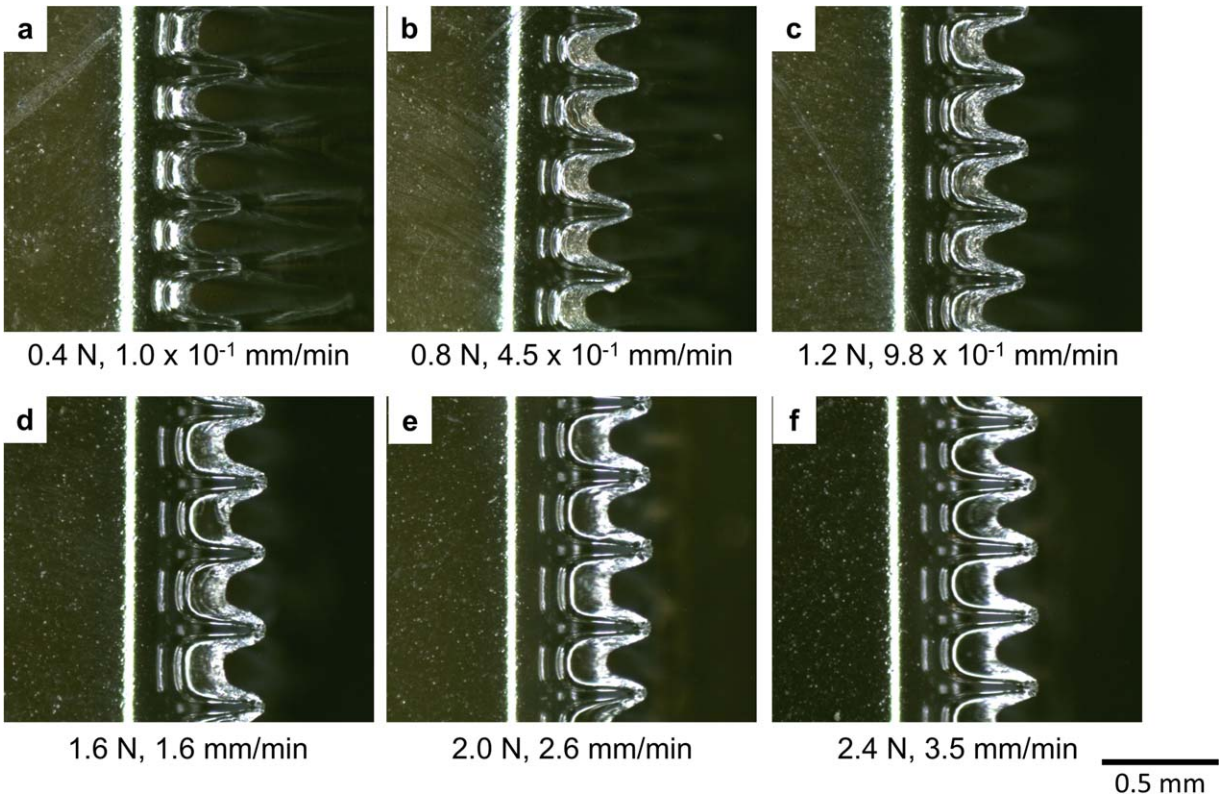

Figure 13. Upper views of stringiness during 90° peeling of crosslinked P(BA–AA) under various peel loads with a constant crosslinker content of 0.008 Eq. The peel load and the actual peel rate are shown under each image. [Color figure can be viewed in the online issue, which is available at wileyonlinelibrary.com.]

Figure 11 shows digital microscope images of the stringiness for PSA with 0.002 Eq. of crosslinker under various peel loads. The peel mode was cohesive failure below 1.2 N and interfacial failure at >2.0 N. The front frame type was observed. Although the length of each protuberance for 0.4 N (a) was equal, it became irregular for peel loads >1.2 N and the difference became more significant with an increase of peel load. Such a phenomenon occurs because the stress dispersion before peeling becomes more insufficient with an increase of the peel rate. Many small branches were observed at the front part of the protuberances and the number of these increased with the peel load. The PSA deforms to disperse the applied stress and this branching occurred as the deformation became more significant with the increase of peel load.

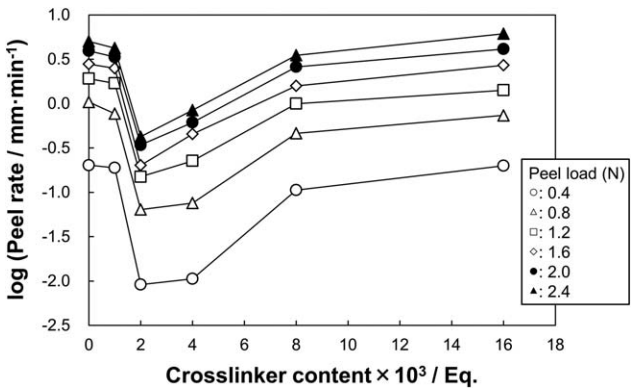

Figure 14. Influence of crosslinker content on the peel rate of crosslinked P(BA–AA) during 90° peeling under various peel loads.

Figure 12 shows digital microscope images of stringiness for the PSA with 0.004 Eq. of crosslinker. The peel mode was interfacial fracture and the front frame type was clearly observed for all peel loads. Some branches were observed for a peel load of 0.4 N (a). The PSA deforms more easily under low peel rate with a low peel load to disperse the applied stress.

Figure 13 shows digital microscope images of stringiness for the PSA with 0.008 Eq. of crosslinker. The peel mode was interfacial fracture and the typical type was clearly observed for all peel loads. There was no significant influence of the peel rate on the stringiness shape. The stringiness for the PSA with 0.016 Eq. of crosslinker was similar to that for 0.008 Eq. (data not shown).

Figure 14 shows the relation between the peel rate (logarithmic) and the crosslinker content. The peel rate was slower for crosslinker contents of 0.002 and 0.004 Eq. for all peel loads. However, the difference in the peel rate with crosslinker content became larger with decreased peel load. Therefore, for comparison of the influence of the PSA properties on the stringiness, a low peel rate is desirable.

Stringiness Length and Width

Side views of the stringiness were also observed under constant peel load (1.2 N) and these are shown in Figure 15. The

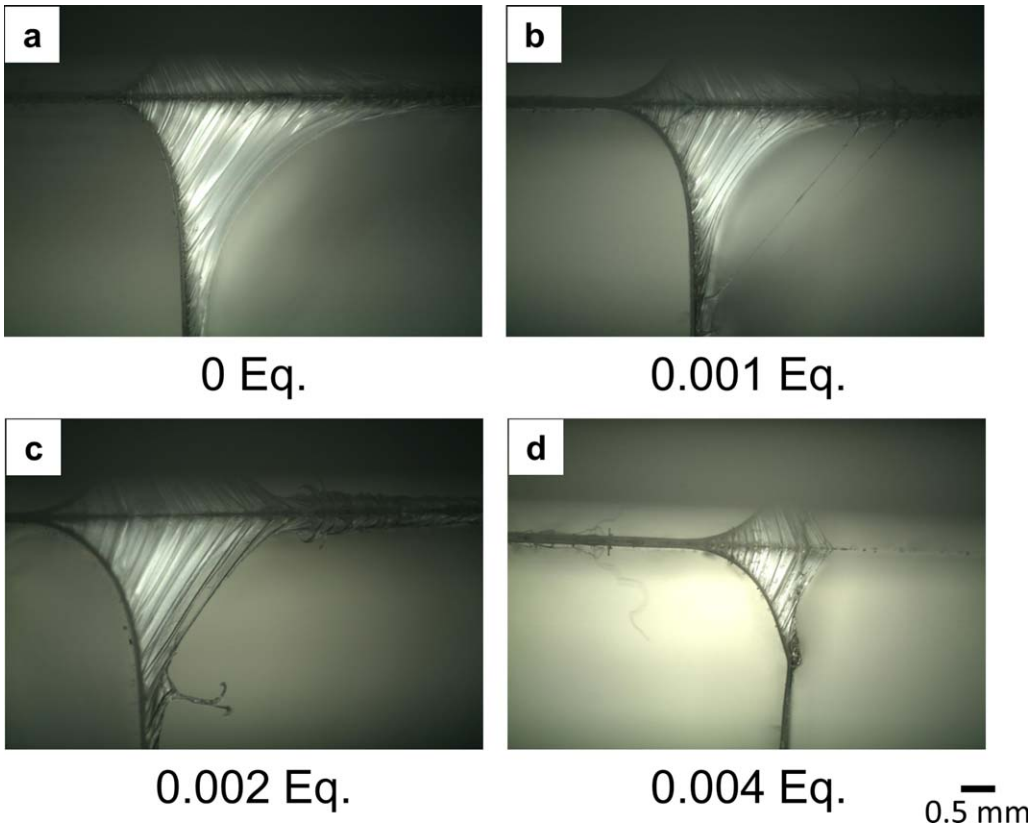

Figure 15. Side views of stringiness during 90° peeling of crosslinked P(BA–AA) with various crosslinker content under a constant peel load of 1.2 N. The crosslinker content is shown under each image. [Color figure can be viewed in the online issue, which is available at wileyonlinelibrary.com.]

stringiness length was larger for 0–0.002 Eq. of crosslinker (a–c), where clear evidence of cohesive failure was observed.

The stringiness length and width [Figure 1(b)] under constant peel load were measured from the side images in Figure 15 and the results are shown in Figure 16. The stringiness length and width were highest for 0.002 Eq. of crosslinker and decreased with an increase of the crosslinker content. These values are also a good index of peel strength.

The stringiness length (L) and width (W) were used to conduct the following analysis. The time required for peeling to progress over distance W is defined as the deformation time (t_d). The peel rate (r_p) is shown as:

$$r_p = \frac{W}{t_d}. \tag{3}$$

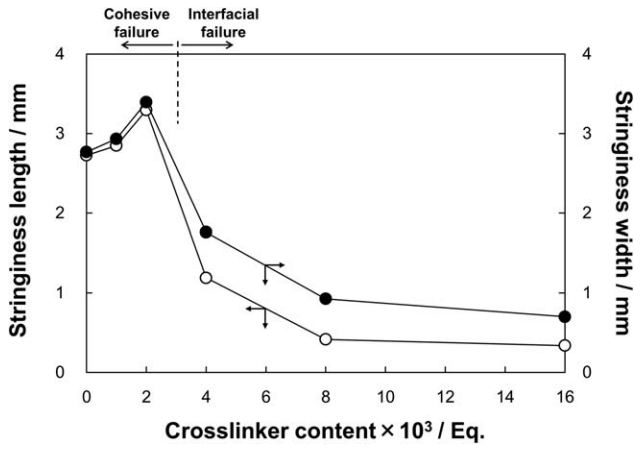

Figure 16. Influences of crosslinker content on the stringiness length and width of crosslinked P(BA–AA) during 90° peeling under a constant peel load of 1.2 N.

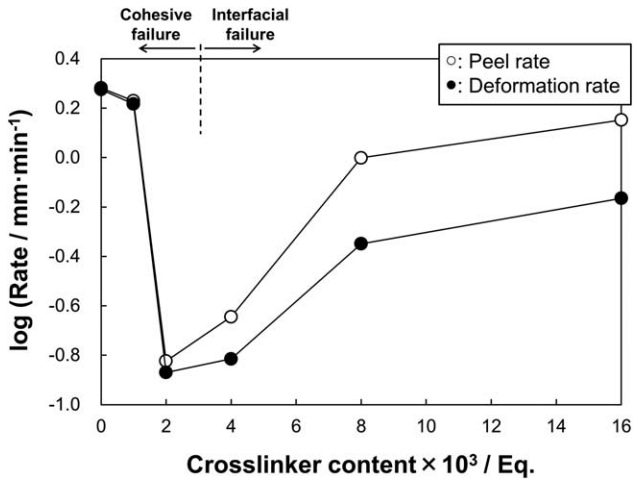

Figure 17. Influence of crosslinker content on the peel rate and deformation rate of crosslinked P(BA–AA) during 90° peeling under a constant peel load of 1.2 N.

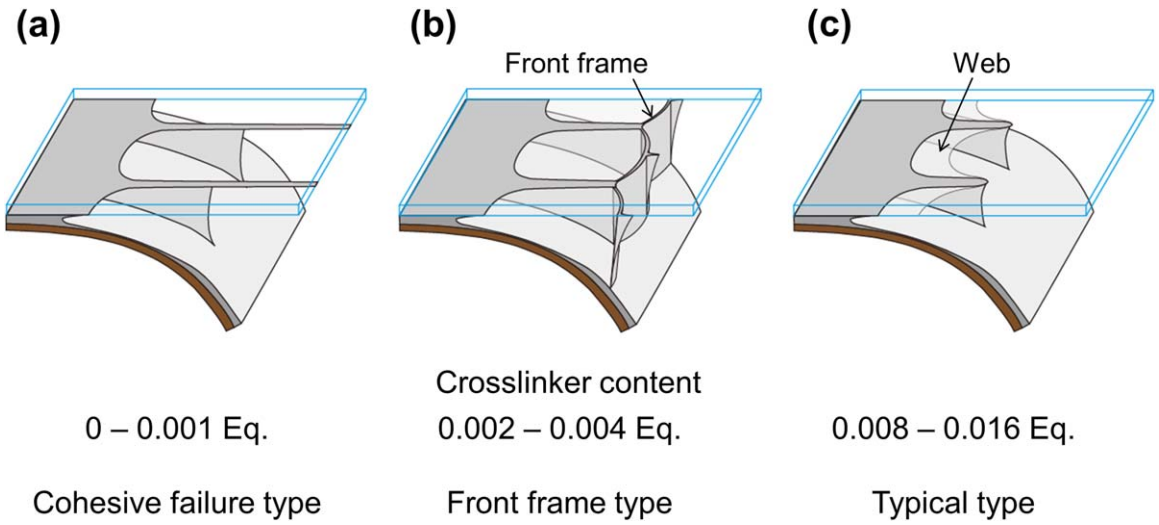

Figure 18. Schematic views of three different types of observed sawtooth-shaped stringiness. [Color figure can be viewed in the online issue, which is available at wileyonlinelibrary.com.]

It was assumed that the t_d is equal to the time that the fibril length extends from 0 to L. The deformation rate (r_d), that is, the rate for the fibril length to extend from 0 to L is shown by:

$$r_d = \frac{L}{t_d}. \quad (4)$$

The influence of the crosslinker content on the peel rate (r_p) and the deformation rate (r_d) under constant peel load is shown in Figure 17. The r_p and r_d were almost the same for crosslinker contents in the range of 0–0.002 Eq., whereas r_p was larger than r_d above 0.004 Eq. The cohesive strength of the PSA increases with the crosslinker content. The PSA has low cohesive strength and high interfacial adhesion, so that the fibril is extended sufficiently before fibril fracture for 0–0.002 Eq. of crosslinker. As a result, r_p and r_d were almost the same. Above 0.004 Eq. of crosslinker, the PSA has larger cohesive strength, that is, resistance to fibril extension. Furthermore, the interfacial adhesion decreases with an increase of the cohesive strength. Therefore, the peeling occurred at the interface, before the fibrils were extended sufficiently.

Difference of Stringiness Shape

The influence of the crosslinker content on the stringiness was observed under constant peel load (Figure 5) and constant peel rate (Figure 9). All observed stringiness was sawtooth-shaped, although the three different types of stringiness were observed, as schematically shown in Figure 18. These types were dependent on the increase of cohesive strength of the PSA with the increase in the degree of crosslinking. On the contrary, the interfacial adhesion decreased with an increase in the degree of crosslinking.

Cohesive Failure Type (a). Belt-like parallel lines remained for crosslinker contents of 0 and 0.001 Eq. The PSA has high interfacial adhesion and low cohesive strength, and thus exhibited cohesive failure.

Front Frame Type (b). Stringiness with a front frame was observed at crosslinker contents of 0.002 and 0.004 Eq. The cohesive strength of these PSAs was higher than that for crosslinker at 0 and 0.001 Eq. This PSA also has sufficient interfacial adhesion and deformability, which result in large internal deformation of the PSA layer. Internal deformation occurs preferentially over peeling and the front frame forms as a result. The peel mode changes from cohesive failure to interfacial failure in this region.

Typical Type (c). The previously reported typical sawtooth-shaped stringiness with interfacial failure was observed at crosslinker contents of 0.008 and 0.016 Eq.[16,17,20–24] Duckfoot-like webbing was also observed. The PSA has high cohesive strength, that is, low interfacial adhesion and deformability. Therefore, peeling progresses with low internal deformation and the PSA forms the typical sawtooth-shaped stringiness as a result.

The shape of stringiness is strongly dependent on the balance between the interfacial adhesion and cohesive strength of the PSA.

CONCLUSIONS

The stringiness of crosslinked P(BA–AA) with various crosslinker contents during 90° peeling was observed under constant peel load and constant peel rate. The influence of the cohesive strength of the PSA on the resulting stringiness was discussed. The following results were obtained.

1. The gel fraction and tensile properties of the PSA were strongly dependent on the crosslinker content. The cohesive strength of PSA was controlled by the degree of crosslinking.
2. All observed stringiness upon peeling was sawtooth-shaped, but it could be classified into three types dependent on the degree of crosslinking: the cohesive failure type, the front frame type, and the typical type. It was found that the shape of stringiness is strongly dependent on the balance between the interfacial adhesion and the cohesive strength of PSA.
3. The stringiness length in the fibril direction and the direction normal to the fibrils, the peel rate under constant peel load, and the peel load required for constant peel rate seem to be good indexes of peel strength.

ACKNOWLEDGMENTS

The authors are grateful to Toagosei Co., Ltd. (Tokyo, Japan) for the polyacrylic polymer preparation and to Mitsubishi Gas Chemical Company, Inc., (Tokyo, Japan) for donation of the crosslinker.

REFERENCES

1. Tse, M. F. *J. Adhes. Sci. Technol.* **1989**, *3*, 551.
2. Yang, H. W. H. *J. Appl. Polym. Sci.* **1989**, *55*, 645.
3. Sasaki, M.; Nakamura, Y.; Fujita, K.; Kinugawa, Y.; Iida, T.; Urahama, Y. *J. Adhes. Sci. Technol.* **2005**, *19*, 1445.
4. Sasaki, M.; Fujita, K.; Adachi, M.; Fujii, S.; Nakamura, Y.; Urahama, Y. *Int. J. Adhes. Adhes.* **2008**, *28*, 372.
5. Nakamura, Y.; Sakai, Y.; Adachi, M.; Fujii, S.; Sasaki, M.; Urahama, Y. *J. Adhes. Sci. Technol.* **2008**, *22*, 1313.
6. Nakamura, Y.; Adachi, M.; Tachibana, Y.; Sakai, Y.; Nakano, S.; Fujii, S.; Sasaki, M.; Urahama, Y. *Int. J. Adhes. Adhes.* **2009**, *29*, 806.
7. Sasaki, M.; Adachi, M.; Kato, Y.; Fujii, S.; Nakamura, Y.; Urahama, Y.; Sakurai, S. *J. Appl. Polym. Sci.* **2010**, *118*, 1766.
8. Nakamura, Y.; Adachi, M.; Kato, Y.; Fujii, S.; Sasaki, M.; Urahama, Y.; Sakurai, S. *J. Adhes. Sci. Technol.* **2011**, *25*, 869.
9. Nakamura, Y.; Adachi, M, Ito, K.; Kato, Y.; Fujii, S.; Sasaki, M.; Urahama, Y.; Sakurai, S. *J. Appl. Polym. Sci.* **2011**, *120*, 2251.
10. Nakamura, Y.; Imamura, K.; Ito, K.; Nakano, S.; Sueoka, A.; Fujii, S.; Sasaki, M.; Urahama, Y. *J. Adhes. Sci. Technol.* **2012**, *26*, 231.
11. Nakamura, Y.; Sakai, Y.; Imamura, K.; Ito, K.; Fujii, S.; Urahama, Y. *J. Appl. Polym. Sci.* **2012**, *123*, 2883.
12. Yamamura, K.; Fujii, S.; Nakamura, Y.; Fujiwara, K.; Hikasa, S.; Urahama, Y. *J. Appl. Polym. Sci.* **2013**, *129*, 1008.
13. Nakamura, Y.; Nakano, S.; Ito, K.; Imamura, K.; Fujii, S.; Sasaki, M.; Urahama, Y. *J. Adhes. Sci. Technol.* **2013**, *27*, 263.
14. Nakamura, Y.; Imamura, K.; Yamamura, K.; Fujii, S.; Urahama, Y. *J. Adhes. Sci. Technol.* **2013**, *27*, 1951.
15. Yamamura, K.; Shitajima, K.; Fujii, S.; Nakamura, Y.; Hamada, Y.; Hagiwara, S.; Kishi, H.; Urahama, Y.; Sasaki, M. *J. Adhes. Sci. Technol.* **2013**, *27*, 2727.
16. Kaelble, D. H. *Trans. Soc. Rheol.* **1965**, *9*, 135.
17. Urahama, Y. *J. Adhes.* **1989**, *31*, 47.
18. Hino, K.; Hashimoto, H. *J. Appl. Polym. Sci.* **1985**, *30*, 3369.
19. Zosel, A. *J. Adhes.* **1989**, *30*, 135.
20. Yamazaki, Y.; Toda, A. *J. Phys. Soc. Jpn.* **2002**, *71*, 1618.
21. Yamazaki, Y.; Toda, A. *J. Phys. Soc. Jpn.* **2004**, *73*, 2342.
22. Miyagi, Z.; Koike, M.; Urahama, Y.; Yamamoto, K. *Int. J. Adhes. Adhes.* **1994**, *14*, 39.
23. Williams, J. A.; Kauzlarich, J. *J. Int. J. Adhes. Adhes.* **2008**, *28*, 192.
24. Vilmin, T.; Ziebert, F.; Raphaël, E. *Langmuir* **2010**, *26*, 3257.